ACCOUNTS
of chemical research

# Interface-Confined Oxide Nanostructures for Catalytic Oxidation Reactions

QIANG FU,* FAN YANG, AND XINHE BAO*

*State Key Laboratory of Catalysis, Dalian Institute of Chemical Physics, Chinese Academy of Sciences, Dalian 116023, P.R. China*

RECEIVED ON AUGUST 23, 2012

## CONSPECTUS

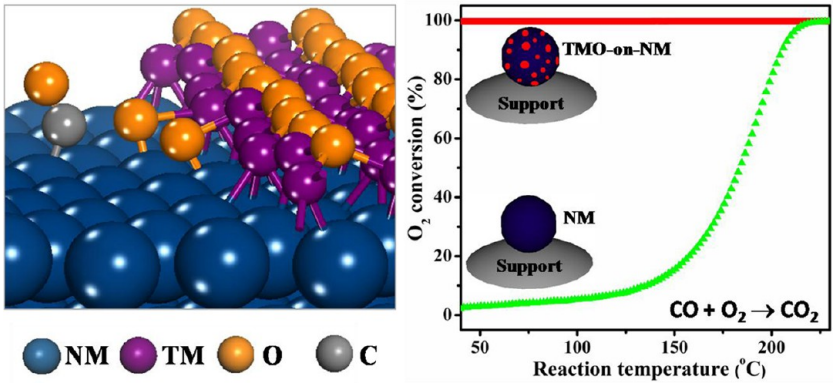


Heterogeneous catalysts, often consisting of metal nanoparticles supported on high-surface-area oxide solids, are common in industrial chemical reactions. Researchers have increasingly recognized the importance of oxides in heterogeneous catalysts: that they are not just a support to help the dispersion of supported metal nanoparticles, but rather interact with supported metal nanoparticles and affect the catalysis. The critical role of oxides in catalytic reactions can become very prominent when oxides cover metal surfaces forming the inverse catalysts.

The source of the catalytic activity in homogeneous catalysts and metalloenzymes is often coordinatively unsaturated (CUS) transition metal (TM) cations, which can undergo facile electron transfer and promote catalytic reactions. Organic ligands and proteins confine these CUS cations, making them highly active and stable. In heterogeneous catalysis, however, confining these highly active CUS centers on an inorganic solid so that they are robust enough to endure the reaction environment while staying flexible enough to perform their catalysis remains a challenge.

In this Account, we describe a strategy to confine the active CUS centers on the solid surface at the interface between a TM oxide (TMO) and a noble metal (NM). Among metals, NMs have high electron negativity and low oxygen affinity. This means that TM cations of the oxide bind strongly to NM atoms at the interface, forming oxygen-terminated-bilayer TMO nanostructures. The resulting CUS sites at the edges of the TMO nanostructure are highly active for catalytic oxidation reactions. Meanwhile, the strong interactions between TMOs and NMs prevent further oxidation of the bilayer TMO phases, which would otherwise result in the saturation of oxygen coordination and the deactivation of the CUS cations. We report that we can also tune the oxide–metal interactions to modulate the bonding of reactants with CUS centers, optimizing their catalytic performance.

We review our recent progress on oxide-on-metal inverse catalysts, mainly the TMO-on-Pt (TM = Fe, Co, and Ni) systems and discuss the interface-confinement effect, an important factor in the behavior of these catalytic systems. We have studied both model catalyst systems and real supported nanocatalysts. Surface science studies and density functional theory calculations in model systems illustrate the importance of the oxide–metal interfaces in the creation and stabilization of surface active centers, and reveal the reaction mechanism at these active sites. In real catalysts, we describe facile preparation processes for fabricating the oxide-on-metal nanostructures. We have demonstrated excellent performance of the inverse catalysts in oxidation reactions such as CO oxidation. We believe that the interface confinement effect can be employed to design highly efficient novel catalysts and that the inverse oxide-on-metal catalysts may find wide applications in heterogeneous catalysis.



Published on the Web 03/04/2013 www.pubs.acs.org/accounts
10.1021/ar300249b 

## Introduction

Heterogeneous catalysts, often consisting of metal nanoparticles (NPs) supported on high-surface-area oxide solids, are widely used in industrial chemical reactions. The importance of oxides in heterogeneous catalysts has been increasingly recognized that they are not just a support to help the dispersion of supported metal NPs. Moreover, they can affect the catalytic process through the interaction with supported metal NPs. In the case of reducible transition metal oxides (TMOs), such interaction can become so prominent that the metal-oxide interface is often considered to play a key role in catalytic reactions.

While our understanding toward the metal−oxide interfaces remains mostly phenomenological, a concept, "strong metal−support interactions" (SMSI), has been regularly used to describe the prominent role that the metal-oxide interface can play in heterogeneous catalysis.[1−4] Introduced by Tauster et al. in the late 1970s,[1,5] SMSI have often been referred to as the effect that reducible oxides, when heated in a reducing environment, migrate onto the surface of metal particles, inhibit the adsorption of reactant molecules, and in certain cases render the metal catalyst unreactive. The process of oxide migration and covering can be reversed when the catalyst is treated in an oxidative environment. In many cases, the SMSI state, that is, metal surfaces covered by oxides, is considered detrimental for catalysis, especially for catalytic oxidation reactions.

Here, we show that, oxides covering metal surfaces, when controlled in a proper way, can be utilized to enhance the catalytic performance. Highly dispersed TMO nanostructures may be deliberately constructed on the surface of NMs, forming oxide-on-metal inverse catalysts. The surface TMO phases are often metastable and two-dimensional (2D), owing to the strong interaction between TM cations and NM atoms underneath.[6−9] TM atoms at the periphery sites of the 2D TMO nanostructures are coordinatively unsaturated, which exhibit extraordinary reactivity and stability in their interaction with reactants.[10,11] Therefore, the TMO-NM interfaces exert a unique chemical environment to confine the active metal centers, which are not in their thermodynamically stable state but can be kinetically trapped at the interface and in certain reaction environments.

In this Account, using the TMO/Pt system as an example, we show that such interface-confined oxide nanostructures can be generally realized through direct synthesis[10,12−14] or catalyst pretreatments.[12,15−17] The inverse catalysts have demonstrated extraordinary performance in low temperature catalytic oxidation reactions. Taking advantage of the interface confinement effect, it is feasible to design highly efficient oxide/metal catalysts and obtain more mechanistic understanding of the role of metal−oxide interfaces in many reactions.

## Oxide-on-Metal Inverse Catalysts

Scheme 1 compares the configuration of conventional oxide-supported metal catalysts with that of oxide-on-metal inverse catalysts. In supported metal catalysts, the density of metal−oxide interfaces is limited by the low contact area between the metal and the oxide (Scheme 1A). To maximize the density of metal−oxide interfaces, highly dispersed TMO nanostructures can be decorated on the surfaces of metal NPs, in which rich boundaries form between TMO surface structures and NM NPs (Scheme 1B).

Most metals have larger surface energy than oxides. According to the Young's equation, $\gamma_{\text{oxide}} = \gamma_{\text{metal}} \cos\theta + \gamma_{\text{interface}}$, it is expected that three-dimensional (3D) nonwetting metal NPs are favored on oxide surfaces,[3,18] whereas oxides tend to wet metal surfaces forming 2D islands (Figure 1). From an atomic view of the metal−oxide interface, multilayer metal nanocrystallites are favored on oxides (Figure 1B). In contrast, oxide nanostructures of monolayer thickness are often observed on metal surfaces (Figure 1D).[6,7,10,19] The planar surfaces of the inverse model systems allow the employment of surface science techniques to obtain an atomic understanding of the structure−reactivity relationship. It has been found that the atomic structure and electronic states of the metal-supported oxides are different from those of their bulk counterparts, resulting in new chemical properties.

**Inverse Model Catalysts.** The inverse model catalysts can be prepared by depositing submonolayer oxide nanostructures on single crystal metal surfaces.[6−11] The growth process consists of the evaporation of TM in an oxygen atmosphere at relatively low substrate temperatures and the subsequent annealing in ultrahigh vacuum (UHV) at elevated temperatures. For example, a 0.25 ML FeO/Pt(111) surface can be prepared by evaporating Fe in $O_2$ ($P_{O_2} = 1.3 \times 10^{-8}$−$1.3 \times 10^{-6}$ mbar) onto a Pt(111) substrate kept at 150−250 K, followed by annealing in UHV up to 673 K.[9] Scanning tunneling microscopy (STM) images (Figure 2A) show that the prepared FeO nanostructures have a uniform thickness and display a Moiré pattern. The FeO nanoislands present a bilayer structure, with the top layer terminated by oxygen atoms and the lower layer composed of iron atoms bonded with Pt atoms.[20] Tunneling spectroscopy taken at the edges of FeO islands shows a distinct electronic state at 0.65 eV above the Fermi level, which can be attributed to the

**SCHEME 1.** Structural Configurations of Conventional Supported Metal Catalysts (A) and the Oxide-on-Metal Inverse Nanocatalysts (B)[a]

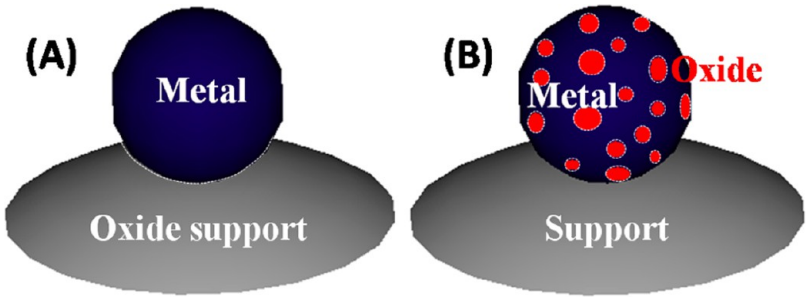


[a]The formed oxide–metal boundaries are marked by dotted lines. With the same amount of metal, the boundary density is much higher in the oxide-on-metal system than that in the oxide–supported metal system.

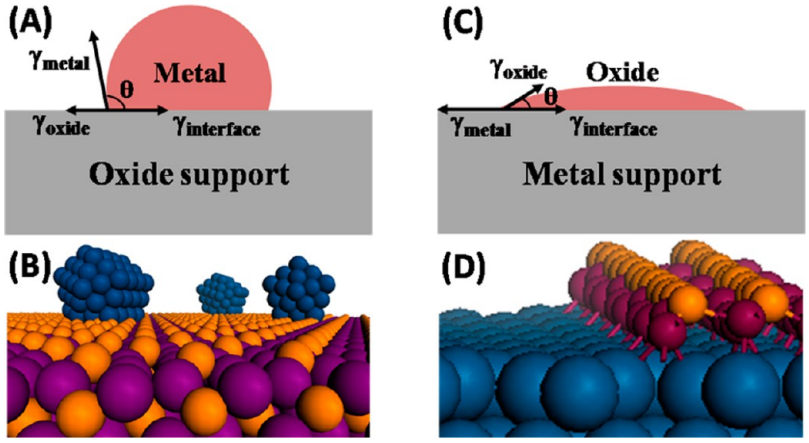


**FIGURE 1.** Schematics of an oxide-supported metal catalyst (A) and an oxide-on-metal inverse catalyst (C). (B) and (D) are the atomic views of the metal-oxide interfaces shown in (A) and (C), respectively. $\gamma_{oxide}$ is the surface energy of oxide, $\gamma_{metal}$ is the surface energy of metal, $\gamma_{interface}$ is the interface free energy, and $\theta$ is the contact angle.

3d state of CUS Fe cations exposed at the boundary sites (Figure 2B).[9] The intensity ratios of XPS peaks, O 1s to Fe2p$_{3/2}$, measured from the FeO nanostructures are always less than that of the full-layer FeO film (Figure 2C). The O/Fe ratio decreases as the density of the island periphery increases, suggesting that oxygen deficiency mainly occurs at the peripheries of the FeO nanostructures.

In comparison, iron oxide was grown on a highly orientated pyrolytic graphite (HOPG) surface using the same growth recipe. The binding energy of Fe 2p$_{3/2}$ of the FeO$_x$/HOPG surface shifted 2.0 eV upward from that of the FeO/Pt(111) surface and is close to that of the stable $Fe_2O_3$ structure. Moreover, 3D NPs instead of 2D islands form on the HOPG surface. The comparison between the growth of iron oxide on Pt(111) and on HOPG surfaces reveals the constraint that the Pt substrate exerts on the formation of monolayer FeO nanoislands.[9]

Similarly, submonolayer NiO or CoO nanostructures can be prepared on Pt(111), which are oxygen-deficient and denoted as TMO$_{1-x}$/Pt(111) (TM = Fe, Co, Ni). For instance, the formed NiO$_{1-x}$ nanoislands are highly dispersed and exhibit planar structure.[21] Besides the Pt(111) substrate, submonolayer TMO nanostructures have also been grown on other precious metal surfaces, such as Ru(0001),[22] Au(111),[23] Ir(100),[24] and Rh(111).[25]

**Inverse Supported Nanocatalysts.** The oxide-on-metal inverse nanocatalysts can be prepared by sequential deposition,[10,26] coimpregnation,[12,15,21,27] or gas-induced surface segregation.[28–31] In the sequential deposition process, supported Pt NPs were first prepared via solution synthesis and then mixed with TM salt solution, for example, Fe(NO$_3$)$_3$, followed by reduction in $H_2$. The formation of TMO$_x$ nanopatches partially covering metal NPs was confirmed by X-ray diffraction (XRD), transmission electron microscopy (TEM) and CO adsorption.[10] Alternatively, TMO$_x$ nanopatches can be deposited on Pt NPs via a reductive deposition precipitation (RDP) process.[32] The deposited TM cations stay exclusively on the surface of Pt NPs, as confirmed by acid leaching together with inductively coupled

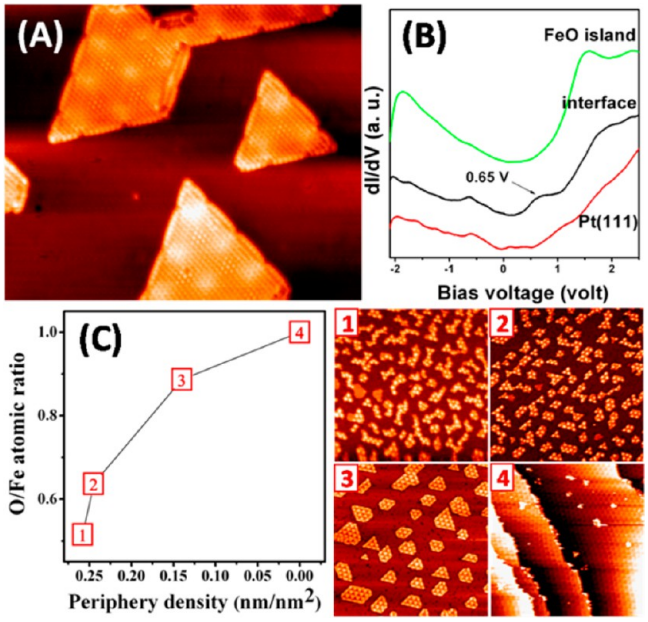


**FIGURE 2.** (A) STM image of FeO nanoislands on Pt(111) (25 nm × 20.8 nm). (B) d*I*/d*V* spectra acquired at 5 K on the surface of FeO islands, at the FeO−Pt interface, and on Pt(111). (C) Ratios of XPS O 1s to Fe $2p_{3/2}$ peak intensity from FeO/Pt(111) surfaces with different periphery density of FeO nanoislands. Samples 1−3 are 0.25 ML FeO nanoislands prepared at $1.3 \times 10^{-6}$ mbar $O_2$ and annealed in UHV at 473, 573, and 673 K, respectively. Sample 4 is the full-monolayer FeO film on Pt(111). The size of STM images are all 100 nm × 100 nm. Reproduced from ref 10.

plasma atomic emission spectrometry measurements.[26] The $TMO_x$-on-Pt (TM = Fe, Co, and Ni) structures can also be synthesized using the coimpregnation process. An inert support, such as silica and carbon black (CB), was mixed with the solutions of Pt and TM precursors and then reduced in $H_2$ at stepwise increasing temperatures. Pt precursors were reduced first, producing Pt NPs. The reduction of TM cations was then facilitated in the presence of Pt NPs, forming $TMO_x$ patches on Pt NPs.[33,34] Finally, $TMO_x$ nanostructures have been grown on Pt surfaces via mild oxidation of Pt-based alloy NPs.[12,27,29−31] The oxidation-induced surface segregation of TM at Au surfaces also produces oxide-on-Au inverse catalysts.[17,35]

The $TMO_x$-on-Pt inverse catalysts were characterized by in situ X-ray absorption near edge structure (XANES) to identify the active structure under reaction conditions. Figure 3A shows the Fe K-edge spectra of a Pt−Fe/CB catalyst exposed to various reaction environments. The pre-edge feature of the Fe K-edge spectra from the Pt−Fe NPs during the preferential oxidation reaction of CO in the presence of $H_2$ (PROX) is located in the middle between those from the reduced and fully oxidized Pt−Fe catalysts, suggesting the presence of low-valent ferrous species under the reaction condition. Thus, the active structure of Pt−Fe NPs during PROX should comprise the Pt-rich core and surface ferrous species, like the structure demonstrated in the FeO/Pt(111) model system. Similarly, the CoO-on-Pt and NiO-on-Pt surface architectures have been identified as the active structures during PROX and CO oxidation in the absence of $H_2$ (COOX).[15,21,27] In addition, recent works have shown that low valent Co,[33,34] Sn,[32,36] and Re[37] (mostly in $TM^{2+}$) species formed in their oxide nanostructures with high reactivity, when in close contact with Pt NPs.

**Interface Confinement Effect.** Both model studies and in situ characterization of supported nanocatalysts reveal that the Pt-supported TMO surface phases have low valent state (mostly in $TM^{2+}$) and planar TM-O structure. Their distinct structural characters should be attributed to the strong interaction between TM cations and Pt atoms underneath. Our density functional theory (DFT) calculations show that the adhesion energy at the FeO/Pt(111) interface is −1.53 eV per FeO formula. The strong bonding between interfacial Fe and Pt atoms can be seen from the extensive orbital hybridization of two elements (Figure 4A).[10,38] The bilayer TMO nanostructures are thermodynamically unstable and, in principle, would favor surface reconstruction in UHV or bind with more oxygen atoms in an oxidative environment. Pt, or a NM with high electron negativity and low oxygen affinity, can form strong interfacial bonds with CUS cations, which rivals the interaction between the NM and oxygen atoms. Subsequently, the formation of interfacial NM−oxygen bonds is prohibited and CUS cations are kinetically stabilized in an oxygen-terminated bilayer TMO nanostructure, remaining undersaturated by oxygen atoms. At the periphery sites of TMO islands, CUS TM atoms exhibit great flexibility in their interaction with reactants. Therefore, the TMO−NM interface demonstrates a unique chemical environment to confine active metal centers with considerable flexibility and stability.

## TMO-on-NM Catalysts for Catalytic Oxidation

**Bifunctional Reaction Mechanism at TMO/Pt Boundary.** We use CO oxidation on TMO/Pt(111) to demonstrate the role of interface-confined oxide nanostructures in catalytic oxidation reactions. CO oxidation on bare Pt-group metal surfaces is usually inhibited by the strong chemisorption of CO, especially when the reactant ratio is stoichiometric or CO rich.[39] On the CO dominant surfaces, the reaction is limited by the adsorption of $O_2$. The presence of interface-confined TMO nanostructures, however, drastically alters the adsorption strength of CO and $O_2$ on the surface.[10,40] DFT calculations show that the adsorption energy of $O_2$ is greatly enhanced at the boundary sites of TMO-Pt(111), rising from −0.77 eV on bare Pt(111) to −1.48 eV at FeO/Pt(111), −1.20 eV at

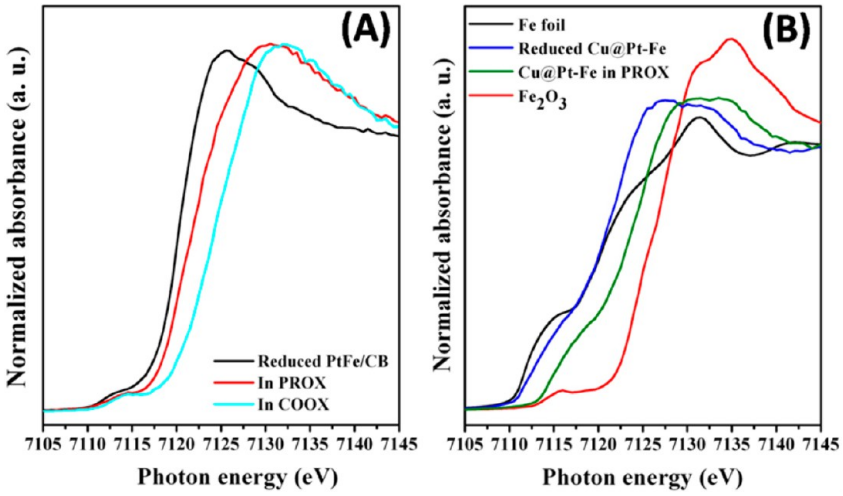


**FIGURE 3.** In situ Fe K-edge XANES spectra of the Pt−Fe/CB (A) and Cu@Pt−Fe/CB (B) catalysts treated at various gaseous environments. Reduction condition: 10% $H_2$ and 90% He; 250 °C. PROX: 1% CO, 0.5% $O_2$, 10% $H_2$, and 88.5% He; room temperature. COOX: 1% CO, 20% $O_2$, and 79% He; room temperature. The spectra from Fe foil and an$Fe_2O_3$ standard are also included.

CoO/Pt(111), and −0.89 eV at NiO/Pt(111). Meanwhile, the adsorption energy of CO is ∼0.1 eV weaker near the boundary sites of TMO/Pt(111) than that on bare Pt(111) (−1.65 eV). Therefore, $O_2$ adsorption on TMO/Pt(111) can compete with the adsorption of CO, given their comparable adsorption energies.

At the TMO/Pt(111) surfaces, the most active sites for $O_2$ dissociation have switched from Pt to the boundaries sites of TMO/Pt; that is, $O_2$ adsorbs on Pt and interacts with the edge sites of TMO. The calculated dissociation barriers at the TMO-Pt boundary (TM = Mn, Fe, Co, Ni, Cu, Zn) are all below 0.22 eV, in contrast to 0.51 eV on bare Pt(111). Meanwhile, the dissociated oxygen atoms coordinate with the CUS cations and the less-reactive Pt atoms (Figure 4B), and thus exhibit modest bonding strength (−1.37 ∼ −1.02 eV/O), which enable the subsequent reaction with the neighboring adsorbed CO to complete the catalytic cycle. Among the 3d group VIIIB TMO/Pt(111) systems, FeO on Pt(111) gives the lowest activation barrier, ∼0.2 eV, for CO oxidation and is thus a suitable candidate for low temperature CO oxidation. Overall, the Pt-cation ensemble at the TMO-Pt boundary provides dual sites for $O_2$ activation and CO adsorption, facilitating the low temperature CO oxidation via a bifunctional mechanism (Figure 4B).[40] Note that, previous studies have invoked that the presence of other reactant molecules, such as $H_2$ or $H_2O$, could open another reaction channel to oxidize CO with hydroxyl groups.[38,41] Similar to the activation of $O_2$, water could dissociate at the step edges of FeO nanostructures producing the hydroxyl groups.[41,42] Our catalytic studies show that adding water to the reactant gases can not improve the activity of CO oxidation, which

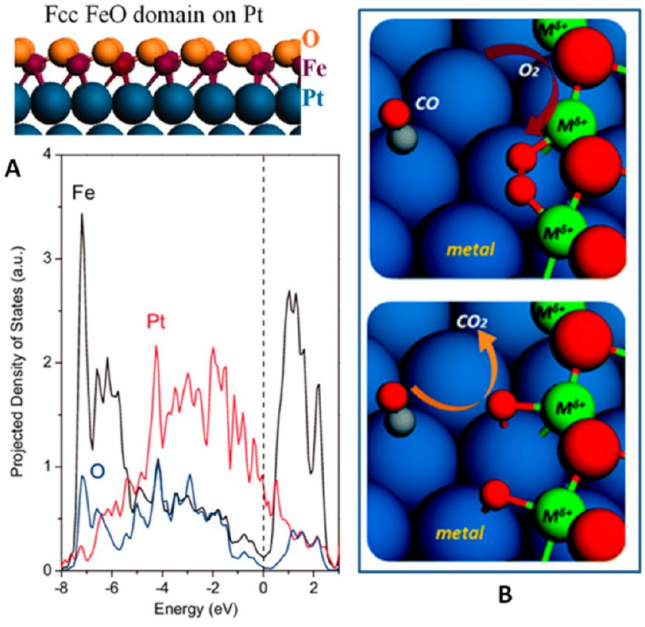


**FIGURE 4.** (A) Projected density of states for interfacial Fe, O, and Pt atoms at fcc domains of FeO overalyer on Pt(111) using $((84)^{1/2} \times (84)^{1/2})$-*R*10.9° − FeO/Pt(111) supercell. (B) Schematic structures of $O_2$ activation and CO oxidation at the TMO/NM(111) boundaries. The initial state of $O_2$ adsorption (up) and the final state of $O_2$ dissociation (down). The blue, red, green, and gray spheres represent NM, O, 3d-TM, and C atoms, respectively.

suggests that the hydroxyl channel might not be a dominant mechanism.

**FeO-on-Pt Structures for PROX.** Figure 5A compares the reactivity for CO oxidation on a few model catalysts, including Pt(111), 0.25 ML Fe/Pt(111), Pt(111) with subsurface Fe, 0.25 ML $FeO_{1-x}$/Pt(111), and Pt(111) covered by 0.25 ML strongly oxidized $FeO_{1+x}$ layer. The reactivity results show

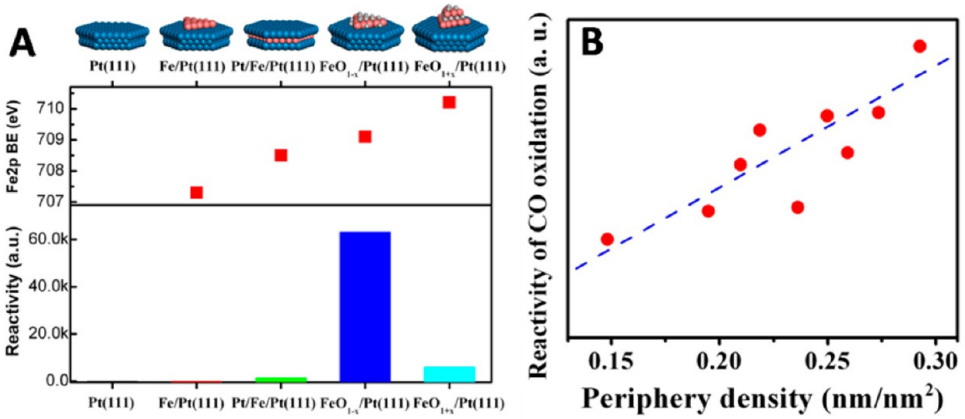


**FIGURE 5.** (A) Reactivity for CO oxidation on the surfaces of Pt(111), 0.25 ML Fe grown on Pt(111) (Fe/Pt(111)), Pt(111) with subsurface Fe (Pt/Fe/Pt(111)), 0.25 ML $FeO_{1-x}$/Pt(111), and Pt(111) covered by 0.25 ML strongly oxidized Fe overlayers ($FeO_{1+x}$/Pt(111)). The corresponding binding energies of Fe 2p are also included. (B) Dependence of reactivity of CO oxidation on the periphery density at 0.25 ML $FeO_{1-x}$/Pt(111) surface. Reproduced from ref 10.

that the $FeO_{1-x}$/Pt(111) surface exhibits the highest activity in CO oxidation. When the Pt(111) surface is fully covered by an FeO layer, there is no CO adsorption at room temperature, thus exhibiting minimal reactivity at this temperature. The FeO film on Pt(111) can however exhibit enhanced activities for CO oxidation at temperatures above 400 K due to the formation of an $FeO_2$ trilayer structure, which is active at high temperatures for the CO oxidation but through the Mars–van Krevelen mechanism.[43]

At the most active 0.25 ML $FeO_{1-x}$/Pt(111) surfaces, we can change the dispersion of FeO nanoislands by varying the growth parameters.[9] The length of the periphery of FeO nanoislands per unit area of the Pt substrate, termed as specific periphery density (SPD), can be varied in a controllable way, though at the same FeO coverage (Figure 2C). When the rate of CO removal was plotted as a function of SPD, a linear correlation between the rate and SPD can be seen (Figure 5B), suggesting that coordinatively unsaturated ferrous (CUF) sites at the edges of the FeO nanoislands are active centers for CO oxidation.[10]

In real catalysts, the reactivity of Pt–Fe (4 wt % Pt/0.5 wt % Fe) NPs supported on CB or silica was tested for PROX and compared to that of the supported Pt (4 wt %) catalyst. For the PROX reaction, CO conversion over the Pt/CB catalyst is negligible around room temperature and increases slowly with temperature. In contrast, the Pt–Fe/CB catalyst exhibits high activity with almost 100% CO conversion and 100% CO selectivity at room temperature (Figure 6), and the FeO-on-Pt surface configuration has been identified as the active structure under the reaction condition (Figure 3A).[10,12] In addition, the Pt–Fe catalysts show no deterioration in their performance after 40 h of reaction at room temperature. When tested under the working condition of a proton exchange membrane fuel

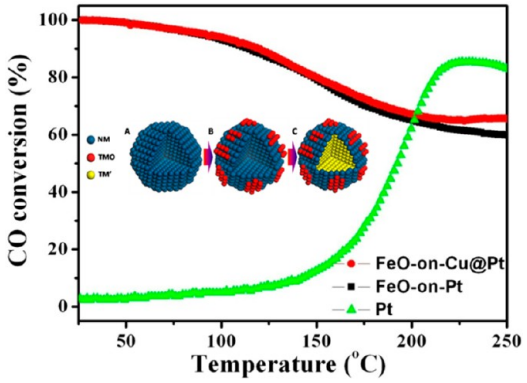


**FIGURE 6.** Temperature-dependent CO conversion of PROX over the 4 wt % Pt/CB, 4 wt % Pt/0.3 wt % Fe/CB, and 1.1 wt % Cu@0.9 wt % Pt/0.1 wt % Fe/CB catalysts (1% CO, 0.5% $O_2$, 50% $H_2$, and 48.5% He; space velocity, 30 000 $mL \cdot g^{-1} \cdot h^{-1}$). The insets illustrate the structures of a Pt NP, an FeO-on-Pt NP, and an FeO-on-Cu@Pt NP.

cell (PEMFC), typically from 353 to 373 K and with 25% $CO_2$ and 20% $H_2O$ in gas, the Pt–Fe catalysts can maintain their excellent performance and yield 92% CO conversion at 353 K.[10] Previous studies have also reported the remarkable PROX activities of Fe oxide-promoted Pt catalysts above 323 K.[13,14] Overall, catalytic studies on the supported Pt–Fe nanocatalysts are in excellent agreement with above model studies on the FeO/Pt(111) surfaces, which clarifies the essential role of surface FeO patches in enhancing the PROX performance.

**FeO-on-Pt Shell Structures for PROX.** Though the Pt–Fe catalyst is an exceptional catalyst, the usage of Pt, 4.0 wt % for instance, is not negligible. To reduce the usage of Pt, we designed a catalyst architecture with a FeO-on-Pt shell grown on a nonprecious metal core. In this architecture, similar interfacial confinement could be imposed on the surface CUF species by the ultrathin Pt film as was done by

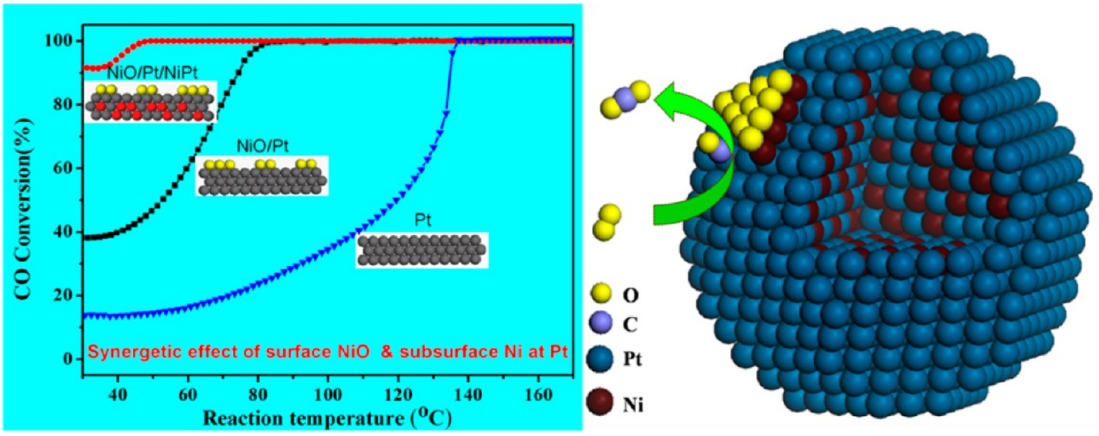


**FIGURE 7.** Temperature-dependent CO conversion in the CO oxidation (1% CO, 20% $O_2$, 79% He; 30 000 mL·$g^{-1}$·$h^{-1}$) over the PtNi/CB catalyst with Ni mainly at the surface and having both surface and subsurface Ni species; for comparison, the result on the Pt/CB catalyst is also included. The right scheme shows the synergetic effect of surface Ni oxide and subsurface Ni species at the Pt–Ni catalysts on the CO oxidation. O, yellow; Ni, brown; Pt, cyan; C, light blue.

bulk Pt.[26] Cu@Pt core–shell NPs were prepared by a sequential polyol deposition process. The Cu@Pt NPs supported on CB were further decorated with Fe via the RDP process, forming the Cu@Pt–Fe/CB catalyst. The K-edge spectrum of the operating Cu@Pt–Fe/CB catalyst in PROX at room temperature indicates the presence of CUF species during reaction (Figure 3B). The FeO-Cu@Pt NP catalyst exhibits extraordinary activity and stability in PROX, similar to those of the FeO-on-Pt NP catalyst (Figure 6).[26] Nonetheless, the Pt loading has been decreased from 4.0 to <1.0 wt % in the FeO-Cu@Pt NP catalyst, using a core–shell nanostructure to support FeO patches.

**NiO-on-Pt and CoO-on-Pt Structures for CO Oxidation.** Pt–Ni and Pt–Co nanocatalysts have been synthesized and tested for PROX and COOX.[15,21,27] Similar to the Pt–Fe catalysts, structural characterization and reaction results suggest that the active catalyst phases consist of Pt NPs decorated with highly dispersed NiO or CoO nanostructures during CO oxidation. The comparative study of the supported $FeO_x$-on-Pt, $CoO_x$-on-Pt, and $NiO_x$-on-Pt nanocatalysts reveals that, in these systems, the active phase for CO oxidation can be unified as the same configuration of TMO-on-Pt (TM = Fe, Co, and Ni). CUS cations at the edge of TMO nanostructure, together with their neighboring Pt atoms, form the active ensembles to catalyze the oxidation reaction via a bifunctional mechanism.

**Synergetic Effect between Surface TMO and Subsurface TM.** Another interesting aspect of the TMO-on-Pt systems is the synergetic effect of surface TM oxide and subsurface TM species in promoting the catalytic activity of the system during CO oxidation. Various well-defined Ni–Pt(111) model catalysts have been constructed and characterized, and combinative STM, XPS, and reactivity studies over these model surfaces show that NiO nanoislands of monolayer thickness on Pt(111) are highly active in $O_2$ dissociation.[21] Meanwhile, the presence of subsurface Ni atoms can substantially weaken the adsorption of CO and O on Pt and subsequently lower the activation barrier for CO + O reaction by a few tenths of eV.[44] Together, a synergetic effect is present between the surface NiO and subsurface Ni species in enhancing the activity of Pt–Ni catalysts for CO oxidation.

The synergetic effect observed in model systems can be translated into real catalysts. Pt–Ni NPs consisting of surface Ni oxide and subsurface Ni were prepared by the one-step coimpregnation process. Reduction of the Pt–Ni NPs in $H_2$ at an intermediate temperature, for example, 250 °C, leads to part of Ni remaining outside of the NP and the rest diffusing to the subsurface region. The PtNi NPs having the $NiO_{1-x}$/Pt/Ni sandwich structure exhibit the highest activity in CO oxidation and 100% CO conversion could be achieved around room temperature (Figure 7).[21] The similar surface architecture consisting of surface TMO and subsurface TM at Pt surface is often produced through reduction at an intermediate temperature. The synergetic role of the surface TMO and subsurface TM has been observed in Pt–Fe,[12] Pt–Co,[27] and Pt–Ni[15,21] catalysts.

## TMO-on-Pt Structures under Various Reaction Conditions

The stabilization of the active TMO nanostructures may rely not only on the confinement at the TMO-NM interface, but also on the gas environment. Reaction studies of the TMO-on-Pt systems in various gases indicate that the TMO nanostructures are sensitive to the reaction environment. For instance, Figure 8 compares the reactivity of the Pt–Fe

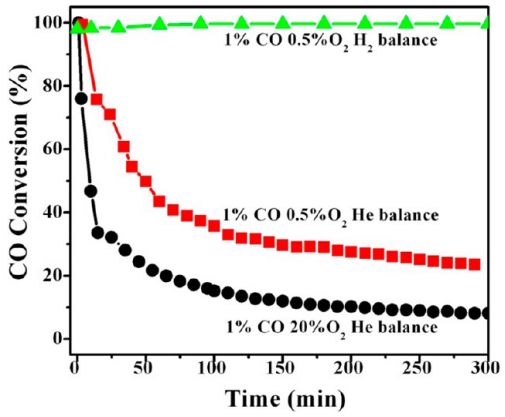


**FIGURE 8.** CO conversion over the Pt–Fe catalyst during various reaction gases.

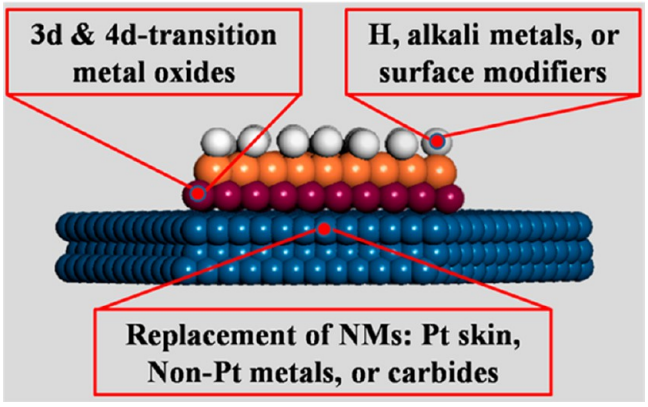


**FIGURE 9.** Perspectives in the inverse TMO-on-NM catalyst systems and the concept of the interface confinement effect.

catalysts during CO oxidations with a variety of CO oxidation gases. The Pt–Fe catalysts deliver the best performance during PROX, showing 100% CO conversion throughout the activity measurements. The activity of the Pt–Fe catalysts drops immediately under the stoichiometric CO oxidation condition without the presence of $H_2$ or when $O_2$ is in excess. The variation of reactivity of the Pt–Fe catalysts demonstrates the critical role of reactants in stabilizing/destabilizing the active FeO-on-Pt structure. During PROX, excess $H_2$ helps to stabilize the active Fe–O bilayer structure, which would otherwise transform into the inactive O–Fe–O trilayer structure in a $H_2$-free environment and deactivates at the reaction temperatures.

Comparing the Pt–Fe, Pt–Co, and Pt–Ni catalysts, the Pt–Fe catalysts exhibit the best activity during PROX and the Pt–Ni catalysts have the best activity during COOX.[27] FeO is most readily to be oxidized in $O_2$-rich gases and thus requires a highly reductive $H_2$-rich environment. NiO, to the contrary, is more difficult to be oxidized and thus can sustain in an oxidative environment. The activity of Pt–Ni catalysts in CO oxidation is enhanced with the increasing $O_2$/CO ratio. Consequently, high CO conversion was observed over the Pt–Ni catalysts for CO oxidation but not during PROX. The CoO-on-Pt structure shows intermediate activity and stability in either CO oxidation or PROX. The trend of reactivity in these TMO-on-Pt structures reflects the different stability of TMO toward oxidation under realistic reaction conditions.[40]

## Conclusions and Perspectives

We have demonstrated that the careful construction of an oxide-on-metal surface structure can enhance the catalytic reactivity of metal catalysts dramatically. In the oxide-on-metal structure, the active oxide phase is two-dimensional, metastable, and highly dispersed, which is confined by the noble metal surface. At the oxide–metal interface, TM cations prefer to bond with NM atoms underneath. Owing to strong interaction between TM and NM, planar TMO nanostructures can be stabilized at the NM surface and TM cations retain their low oxygen coordination numbers. Particularly, TM cations exposed at the edges of TMO nanostructures are coordinatively flexible and become highly active in the dissociative adsorption of molecules, for example, $O_2$ and $H_2O$. The bonding of dissociated oxygen atom with the interfacial NM-TM atoms is modest, leading to facile oxidation reactions at low temperature. The active NM-$TM_{cus}$-O complex at the boundary of TMO and NM provides dual sites for catalytic reactions.

Studies in NM catalysts supported on reducible oxides have shown that surface defects of the oxides, oxygen vacancies in particular, play a key role in anchoring active NM NPs.[3,45] At the oxygen vacancy, NM atoms are bonded with CUS cations of the oxide, forming the active NM-$TM_{cus}$-O complexes at the perimeters of NM NPs,[3,46,47] similar to those at the perimeters of TMO nanostructures in the TMO-on-NM systems. Interestingly, the bifunctional reaction mechanism has been identified to dominate oxidation reactions occurring on oxide supported NM catalysts as well.[47,48] Given these similarities, the formation of active NM-$TM_{cus}$-O structural complexes might be widely present not only in inverse catalysts, but also in metal catalysts supported on reducible oxides. In this sense, the effect of interface confinement could be used to optimize the catalytic performance of a variety of metal-oxide composite systems and should be of great importance for heterogeneous catalysis.

The effect of interface confinement remains to be explored in more catalytic systems and can be used in the design of novel catalysts (Figure 9). First, candidates for the supported

TMO nanostructures may be further extended from 3d TMO to 4d and rare earth TM oxides. The hybridization between f electrons of rare earth metal with d electrons of NM might yield novel properties at the TMO/NM interface. Another question would be whether we can tune the interfacial interaction, or adjust the confinement effect, through surface functionalization of the oxide. The modulation of interface confinement would allow the catalytic system to be applied to more complex reactions and to increase the selectivity of catalysts. Finally, can we replace the precious metal component in the TMO-on-NM system with nonprecious component? We have described a method to lower the usage of Pt via deposition of FeO nanostructures on Pt shell or Pt skin surfaces.[26] Moreover, the active surface oxide phases can be confined on Au surface, producing highly active TMO-on-Au catalytic systems.[16,17] A major challenge now becomes whether we can replace fully the precious metal component with nonprecious elements or composites. It has been speculated that carbides and nitrides could exhibit a NM-like electronic structure near the Fermi edge. Future attempts to construct TMO-on-carbide or TMO-on-nitride would allow us to answer this question.

*This work was financially supported by the National Natural Science Foundation of China (Grants 11079005, 21103171, and 21103181), Ministry of Science and Technology of China (Grants 2011CBA00503 and 2012CB215500), and Chinese Academy of Sciences ("Bairen" program). We thank fruitful discussions with Profs. Weixue Li and Ding Ma.*

## BIOGRAPHICAL INFORMATION

**Qiang Fu** received his bachelor degree and doctorate of chemistry from Beijing Institute of Technology in 1996 and 2000, respectively. Between 2000 and 2006, he worked as a postdoctoral fellow in Max Planck Institute for Metal Research and Max Planck Society of Fritz Haber Institute. In 2006, he joined Dalian Institute of Chemical Physics, the Chinese Academy of Sciences (CAS), sponsored by the 100-Talents program of CAS. He was promoted as a full professor in 2008. His current research interest is surface and interface catalysis.

**Fan Yang** received his Ph.D. in Chemistry from Texas A&M University in 2007, under the guidance of Prof. Wayne Goodman. After a short stay in Wayne's group as a postdoc, he joined Brookhaven National Laboratory in 2008 to work with Dr. Jose Rodriguez and Dr. Dario Stacchiola. In 2012, he joined the group led by Prof. Xinhe Bao in Dalian Institute of Chemical Physics as a staff member. His research interest is in the fields of surface science and catalysis.

**Xinhe Bao** received his Ph.D. in Physical Chemistry from Fudan University in 1987. He held an Alexander von Humboldt Research Fellow position in Fritz-Haber Institute between 1989 and 1995, hosted by Prof. Gerhard Ertl. Following that, he joined Dalian Institute of Chemical Physics as a full Professor. He became a member of the Chinese Academy of Sciences in 2009. His research interest is nano and interfacial catalysis, focusing on the fundamental understanding of heterogeneous catalysis.

## FOOTNOTES

*To whom correspondence should be addressed. E-mail: qfu@dicp.ac.cn (Q.F.); xhbao@dicp.ac.cn (X.B.).

The authors declare no competing financial interest.

## REFERENCES

1 Tauster, S. J.; Fung, S. C.; Garten, R. L. Strong metal-support interactions. Group 8 noble metals supported on titanium dioxide. *J. Am. Chem. Soc.* **1978**, *100*, 170–175.

2 Haller, G. L.; Resasco, D. E. Metal support interaction - group-VIII metals and reducible oxides. *Adv. Catal.* **1989**, *36*, 173–235.

3 Fu, Q.; Wagner, T. Interaction of nanostructured metal overlayers with oxide surfaces. *Surf. Sci. Rep.* **2007**, *62*, 431–498.

4 Goodman, D. W. "Catalytically active Au on titania": yet another example of a strong metal support interaction(SMSI)? *Catal. Lett.* **2005**, *99*, 1–4.

5 Tauster, S. J. Strong metal-support interactions. *Acc. Chem. Res.* **1987**, *20*, 389–394.

6 Netzer, F. P.; Allegretti, F.; Surnev, S. Low-dimensional oxide nanostructures on metals: Hybrid systems with novel properties. *J. Vac. Sci. Technol., B* **2010**, *28*, 1–16.

7 Rodriguez, J. A.; Hrbek, J. Inverse oxide/metal catalysts: A versatile approach for activity tests and mechanistic studies. *Surf. Sci.* **2010**, *604*, 241–244.

8 Hayek, K.; Fuchs, M.; Klotzer, B.; Reichl, W.; Rupprechter, G. Studies of metal-support interactions with "real" and "inverted" model systems: reactions of CO and small hydrocarbons with hydrogen on noble metals in contact with oxides. *Top. Catal.* **2000**, *13*, 55–66.

9 Yao, Y. X.; Fu, Q.; Wang, Z.; Tan, D. L.; Bao, X. H. Growth and characterization of two-dimensional FeO nanoislands supported on Pt(111). *J. Phys. Chem. C* **2010**, *114*, 17069–17079.

10 Fu, Q.; Li, W. X.; Yao, Y. X.; Liu, H. Y.; Su, H. Y.; Ma, D.; Gu, X. K.; Chen, L. M.; Wang, Z.; Zhang, H.; Wang, B.; Bao, X. H. Interface-confined ferrous centers for catalytic oxidation. *Science* **2010**, *328*, 1141–1144.

11 Rodriguez, J. A.; Ma, S.; Liu, P.; Hrbek, J.; Evans, J.; Perez, M. Activity of CeOx and TiOx nanoparticles grown on Au(111) in the water-gas shift reaction. *Science* **2007**, *318*, 1757–1760.

12 Xu, H.; Fu, Q.; Yao, Y. X.; Bao, X. H. Highly active Pt-Fe bicomponent catalysts for CO oxidation in the presence and absence of $H_2$. *Energy Environ. Sci.* **2012**, *5*, 6313–6320.

13 Liu, X. S.; Korotkikh, O.; Farrauto, R. Selective catalytic oxidation of CO in $H_2$: structural study of Fe oxide-promoted Pt/alumina catalyst. *Appl. Catal., A* **2002**, *226*, 293–303.

14 Kotobuki, M.; Watanabe, A.; Uchida, H.; Yamashita, H.; Watanabe, M. Reaction mechanism of preferential oxidation of carbon monoxide on Pt, Fe, and Pt-Fe/mordenite catalysts. *J. Catal.* **2005**, *236*, 262–269.

15 Mu, R. T.; Guo, X. G.; Fu, Q.; Bao, X. H. Oscillation of surface structure and reactivity of PtNi bimetallic catalysts with redox treatments at variable temperatures. *J. Phys. Chem. C* **2011**, *115*, 20590–20595.

16 Zhou, S. H.; Yin, H. F.; Schwartz, V.; Wu, Z. L.; Mullins, D.; Eichhorn, B.; Overbury, S. H.; Dai, S. In situ phase separation of NiAu alloy nanoparticles for preparing highly active Au/NiO CO oxidation catalysts. *ChemPhysChem* **2008**, *9*, 2475–2479.

17 Liu, X. Y.; Liu, M. H.; Luo, Y. C.; Mou, C. Y.; Lin, S. D.; Cheng, H. K.; Chen, J. M.; Lee, J. F.; Lin, T. S. Strong metal-support interactions between gold nanoparticles and ZnO nanorods in CO oxidation. *J. Am. Chem. Soc.* **2012**, *134*, 10251–10258.

18 Campbell, C. T. Ultrathin metal films and particles on oxide surfaces: Structural, electronic and chemisorptive properties. *Surf. Sci. Rep.* **1997**, *27*, 1–111.

19 Schoiswohl, J.; Surnev, S.; Sock, M.; Ramsey, M. G.; Kresse, G.; Netzer, F. R. Thermodynamically controlled self-assembly of two-dimensional oxide nanostructures. *Angew. Chem., Int. Ed.* **2004**, *43*, 5546–5549.

20 Weiss, W.; Ranke, W. Surface chemistry and catalysis on well-defined epitaxial iron-oxide layers. *Prog. Surf. Sci.* **2002**, *70*, 1–151.

21 Mu, R. T.; Fu, Q.; Xu, H.; Zhang, H. I.; Huang, Y. Y.; Jiang, Z.; Zhang, S. O.; Tan, D. L.; Bao, X. H. Synergetic effect of surface and subsurface Ni species at Pt-Ni bimetallic catalysts for CO oxidation. *J. Am. Chem. Soc.* **2011**, *133*, 1978–1986.

22 Ketteler, G.; Ranke, W. Heteroepitaxial growth and nucleation of iron oxide films on Ru(0001). *J. Phys. Chem. B* **2003**, *107*, 4320–4333.

23 Khan, N. A.; Matranga, C. Nucleation and growth of Fe and FeO nanoparticles and films on Au(111). *Surf. Sci.* **2008**, *602*, 932–942.

24 Ebensperger, C.; Gubo, M.; Meyer, W.; Hammer, L.; Heinz, K. Substrate-induced structural modulation of a CoO(111) bilayer on Ir(100). *Phys. Rev. B* **2010**, *81*, 235405.

25 Franz, T.; Zabloudil, J.; Mittendorfer, F.; Gragnaniello, L.; Parteder, G.; Allegretti, F.; Surnev, S.; Netzer, F. P. Deformed surface oxides: uncommon structure of a(6 × 1) NiO surface oxide on Rh(111). *J. Phys. Chem. Lett.* **2012**, *3*, 186–190.

26 Guo, X. G.; Fu, Q.; Ning, Y. X.; Wei, M. M.; Li, M. R.; Zhang, S.; Jiang, Z.; Bao, X. H. Ferrous centers confined on core-Shell nanostructures for low temperature CO oxidation. *J. Am. Chem. Soc.* **2012**, *134*, 12350–12353.

27 Xu, H.; Fu, Q.; Guo, X. G.; Bao, X. H. Architecture of Pt-Co bimetallic catalysts for catalytic CO oxidation. *ChemCatChem* **2012**, *4*, 1645–1652.

28 Mu, R. T.; Fu, Q.; Liu, H. Y.; Tan, D. L.; Zhai, R. S.; Bao, X. H. Reversible surface structural changes in Pt-based bimetallic nanoparticles during oxidation and reduction cycles. *Appl. Surf. Sci.* **2009**, *255*, 7296–7301.

29 Ma, T.; Fu, Q.; Su, H. Y.; Liu, H. Y.; Cui, Y.; Wang, Z.; Mu, R. T.; Li, W. X.; Bao, X. H. Reversible structural modulation of Fe-Pt bimetallic surfaces and its effect on reactivity. *ChemPhysChem* **2009**, *10*, 1013–1016.

30 Ma, T.; Fu, Q.; Cui, Y.; Zhang, Z.; Wang, Z.; Tan, D. L.; Bao, X. H. Controlled transformation of the structures of surface Fe(FeO) and subsurface Fe on Pt(111). *Chin. J. Catal.* **2010**, *31*, 24–32.

31 Su, H. Y.; Gu, X. K.; Ma, X. F.; Zhao, Y. H.; Bao, X. H.; Li, W. X. Structure evolution of Pt-3d transition metal alloys under reductive and oxidizing conditions and effect on the CO oxidation: a first-principles study. *Catal. Today* **2011**, *165*, 89–95.

32 Plomp, A. J.; van Asten, D. M. P.; van der Eerden, A. M. J.; Maki-Arvela, P.; Murzin, D. Y.; de Jong, K. P.; Bitter, J. H. Catalysts based on platinum-tin and platinum-gallium in close contact for the selective hydrogenation of cinnamaldehyde. *J. Catal.* **2009**, *263*, 146–154.

33 Papaefthimiou, V.; Dintzer, T.; Dupuis, V.; Tamion, A.; Tournus, F.; Teschner, D.; Havecker, M.; Knop-Gericke, A.; Schlogl, R.; Zafeiratos, S. When a metastable oxide stabilizes at the nanoscale: wurtzite CoO formation upon dealloying of PtCo nanoparticles. *J. Phys. Chem. Lett.* **2011**, *2*, 900–904.

34 Zheng, F.; Alayoglu, S.; Guo, J. H.; Pushkarev, V.; Li, Y. M.; Glans, P. A.; Chen, J. L.; Somorjai, G. In-situ x-ray absorption study of evolution of oxidation states and structure of cobalt in Co and CoPt bimetallic nanoparticles(4 nm) under reducing($H_2$) and oxidizing($O_2$) Environments. *Nano Lett.* **2011**, *11*, 847–853.

35 Liu, X. Y.; Wang, A. Q.; Li, L.; Zhang, T.; Mou, C. Y.; Lee, J. F. Structural changes of Au-Cu bimetallic catalysts in CO oxidation: In situ XRD, EPR, XANES, and FT-IR characterizations. *J. Catal.* **2010**, *278*, 288–296.

36 Zhou, W. P.; Axnanda, S.; White, M. G.; Adzic, R. R.; Hrbek, J. Enhancement in ethanol electrooxidation by $SnO_x$ nanoislands grown on Pt(111): effect of metal oxide-metal interface sites. *J. Phys. Chem. C* **2011**, *115*, 16467–16473.

37 Ishida, Y.; Ebashi, T.; Ito, S.; Kubota, T.; Kunimori, K.; Tomishige, K. Preferential CO oxidation in a $H_2$-rich stream promoted by $ReO_x$ species attached to Pt metal particles. *Chem. Commun.* **2009**, 5308–5310.

38 Gu, X. K.; Ouyang, R. H.; Sun, D. P.; Su, H. Y.; Li, W. X. CO oxidation at the perimeters of an FeO/Pt(111) interface and how water promotes the activity: a first-principles study. *ChemSusChem* **2012**, *5*, 871–878.

39 Berlowitz, P. J.; Peden, C. H. F.; Goodman, D. W. Kinetics of CO oxidation on single-crystal Pd, Pt, and Ir. *J. Phys. Chem.* **1988**, *92*, 5213–5221.

40 Sun, D. P.; Gu, X. K.; Ouyang, R. H.; Su, H. Y.; Fu, Q.; Bao, X. H.; Li, W. X. Theoretical study of the role of a metal-cation ensemble at the oxide-metal boundary on CO oxidation. *J. Phys. Chem. C* **2012**, *116*, 7491–7498.

41 Xu, L. S.; Ma, Y. S.; Zhang, Y. L.; Jiang, Z. Q.; Huang, W. X. Direct evidence for the interfacial oxidation of CO with hydroxyls catalyzed by Pt/oxide nanocatalysts. *J. Am. Chem. Soc.* **2009**, *131*, 16366–16367.

42 Wang, W.; Zhang, H.; Wang, W. H.; Zhao, A. D.; Wang, B.; Hou, J. G. Observation of water dissociation on nanometer-sized FeO islands grown on Pt(111). *Chem. Phys. Lett.* **2010**, *500*, 76–81.

43 Sun, Y. N.; Qin, Z. H.; Lewandowski, M.; Carrasco, E.; Sterrer, M.; Shaikhutdinov, S.; Freund, H. J. Monolayer iron oxide film on platinum promotes low temperature CO oxidation. *J. Catal.* **2009**, *266*, 359–368.

44 Su, H. Y.; Bao, X. H.; Li, W. X. Modulating the reactivity of Ni-containing Pt(111)-skin catalysts by density functional theory calculations. *J. Chem. Phys.* **2008**, *128*, 194707.

45 Wahlstrom, E.; Lopez, N.; Schaub, R.; Thostrup, P.; Ronnau, A.; Africh, C.; Laegsgaard, E.; Norskov, J. K.; Besenbacher, F. Bonding of gold nanoclusters to oxygen vacancies on rutile $TiO_2$(110). *Phys. Rev. Lett.* **2003**, *90*, 26101.

46 Fujitani, T.; Nakamura, I.; Akita, T.; Okumura, M.; Haruta, M. Hydrogen dissociation by gold clusters. *Angew. Chem., Int. Ed.* **2009**, *48*, 9515–9518.

47 Liu, H.; Kozlov, A. I.; Kozlova, A. P.; Shido, T.; Asakura, K.; Iwasawa, Y. Active oxygen species and mechanism for low-temperature CO oxidation reaction on a $TiO_2$-supported Au catalyst prepared from Au($PPh_3$)($NO_3$) and As-precipitated titanium hydroxide. *J. Catal.* **1999**, *185*, 252–264.

48 Green, I. X.; Tang, W.; Neurock, M.; Yates, J. T. Spectroscopic observation of dual catalytic sites during oxidation of CO on a Au/$TiO_2$ catalyst. *Science* **2011**, *333*, 736–739.